Published in final edited form as:
Neurosci Lett. 2013 March 22; 538: 26–31. doi:10.1016/j.neulet.2013.01.027.

Differential Molecular Chaperone Response Associated with Various Mouse Adapted Scrapie Strains

Ayodeji A. Asuni[1,*], **Joanna E. Pankiewicz**[3,1], and **Martin J. Sadowski**[1,2,3,*]

[1]Department of Neurology, New York University School of Medicine, New York, NY 10016, USA

[2]Department of Psychiatry, New York University School of Medicine, New York, NY 10016, USA

[3]Department of Biochemistry & Molecular Pharmacology, New York University School of Medicine, New York, NY 10016, USA

Abstract

Prionoses are a group of neurodegenerative diseases characterized by misfolding of cellular prion protein (PrP^C) and accumulation of its diseases specific conformer PrP^{Sc} in the brain and neuropathologically, they can be associated with presence or absence of PrP amyloid deposits. Functional molecular chaperones (MCs) that constitute the unfolded protein response include heat shock proteins and glucose-regulated protein families. They protect intracellular milieu against various stress conditions including accumulation of misfolded proteins and oxidative stress, typical of neurodegenerative diseases. Little is known about the role of MCs in pathogenesis of prionoses in mammalian prion model systems. In this study we characterized MCs response pattern in mice infected with various mouse adapted scrapie strains. Rather than uniform upregulation of MCs, we encountered two distinctly different patterns of MCs response distinguishing ME7 and 87V strains from 22L and 139A strains. ME7 and 87V strains are known for the induction of amyloid deposition in infected animals, while in mice infected with 22L and 139A strains amyloid deposits are absent. MCs response pattern similar to that associated with amyloidogenic ME7 and 87V strains was also observed in APPPS1-21 Alzheimer's transgenic mice, which represent an aggressive model of cerebral amyloidosis caused by β-amyloid deposition. Our results highlight the probability that different mechanisms of MCs regulation exist driven by amyloidogenic and non-amyloidogenic nature of prion strains.

1. Introduction

Accumulation of misfolded proteins is an underlying feature of several neurodegenerative diseases, including Alzheimer's disease (AD), tauopathies, Parkinson's disease, polyglutamine diseases, and prion disease (prionoses). Prionoses are characterized by the conformational conversion of cellular prion protein (PrP^C) to its toxic and proteinase K (PK) resistant conformer (PrP^{Sc}). Furthermore, PrP^{Sc} shows reduced solubility and inherent propensity to self-assembly into oligomeric and fibrillar structures. Accumulation of PrP^{Sc} is associated with widespread neurodegeneration; with hallmarks including spongiform

*Corresponding authors: Dr. Martin J. Sadowski and Dr. Ayodeji A. Asuni, New York University School of Medicine, 450E 29th St., Room 830, New York, NY 10016, Telephone: (212)263-0984, Facsimile: (646)501-4501, sadowm01@med.nyu.edu (M.J.S.) and asuni@mac.com (A.A.A.).

changes, intraneuronal vacuolization, astrogliosis, loss of synapses and neuronal bodies; however, Thioflavin-S positive amyloid plaques composed of PrP fragments are present only in a subset of prionoses (reviewed in [9]). Prion strains are defined as clinically and neuropathologically distinct phenotypes of prion disease within given species, with features that can be precisely replicated after transmission. Multiple prion strains have been described in sheep and transmitted into mice resulting in generation of mouse adapted scrapie strains [4]. Examples of mouse adapted prion strains include ME7 and 87V, which among other distinguishing phenotypical features both show propensity for PrP amyloid deposition and 139A and 22L in which amyloid deposits are absent [4;6;8].

Elucidating the mechanisms by which misfolded proteins induce neurodegeneration requires information about their relationship with the protein quality control system that chaperones protein folding for proper function, refolds their misfolded conformers, or directs them for degradation. This protein quality control system also dubbed as molecular chaperones (MCs) encompasses two large protein families the heat shock proteins (HSP) and the glucose-regulated proteins [Grp], reviewed in [15]. The HSPs are a family of structurally related proteins classified by their molecular weights including HSP20, HSP40, HSP60, HSP70, HSP90, and HSP100, which are expressed in the cytoplasm, except for Hsp60 which has primarily mitochondrial localization. The Grp family includes Grp58, Grp78, and Grp94 proteins, which are expressed in the endoplasmic reticulum (ER) and are involved in primary folding of nascent proteins translated in the ER. They also serve as ER stress markers in conditions of disturbed proteostasis where they regulate unspecific aggregation and target misfolded proteins for proteasome-mediated degradation (reviewed in [21]).

The role of MCs in the pathogenesis of several neurodegenerative diseases associated with abnormal protein folding has been extensively studied (reviewed in [10]), while information about the role of MCs in mammalian prion model systems has been fragmentary [2;3;12;13;23]. Herein we examined whether a selection of MCs, that collectively represent the major MCs systems protecting neurons against protein unfolding and aggregation, are involved in pathogenesis of various mouse adapted scrapie strains. We provide evidence that amyloidogenic and non-amyloidogenic prion strains engage MCs response differently, which may significantly contribute to phenotypic differences observed among prion strains.

2. Material and Methods

2.1. Animals

Animal experiments were carried out in accordance with the National Institutes of Health guide for the care of laboratory animals and were approved by the Institutional Animal Care and Use Committee. All efforts were made to minimize animal suffering and reduce the number of animals used. This study was performed on the material archived during our previous studies, which encompassed brain hemispheres flash-frozen at the autopsy and stored at −80°C and corresponding brain hemispheres embedded in paraffin blocks. All brains selected for this were collected within a period of four months and stored for approximately two years prior to commencing this work. We included brain tissue from female CD-1 mice intraperitoneally inoculated with ME7, 22L, 139A mouse adapted scrapie strains [19], control CD-1 mice inoculated with normal brain homogenate (NBH), female MB mice inoculated with 87V strain [18] and female APPPS1-21 transgenic (Tg) mice model of Alzheimer's disease (AD) [17] six of each. All prion inoculated mice were killed in the advanced stage of the disease when they were unable to reach the food bin or water spout or regain posture after being placed on their side. For mice inoculated with ME7, 22L, 139A strains the survival period ranged from 26 to 30 weeks, for mice inoculated with 87V strain it ranged from 38 to 42 weeks, while the control mice remained neurologically intact and were killed 30 weeks following NBH inoculation. APPPS1-21 AD Tg mice overexpress

a sequence of human amyloid precursor protein with the double Swedish mutation KM670/671NL and a sequence of human presenilin 1 with the L166P mutation under the control of a neuron-specific Thy1 promoter [17]. APPPS1-21 mice represent one of the most aggressive models of β-amyloid (Aβ) deposition and in these mice the first Thioflavin-S binding Aβ plaques form during the second month of their life. We analyzed brains of APPPS1-21 mice killed at the age of two and eight months old, which both showed no neurological symptoms indicating motor or coordination impairment.

2.2. Western Immunoblotting and Densitometric Analysis

Frozen brain hemispheres were thawed, weighed, and homogenized for downstream biochemical analyses following our published protocols [19]. Protein concentration in the brain homogenate was determined using the bicinchoninic acid method. For PrP^{Sc} analysis aliquots of brain homogenates containing 20μg of the total protein were PK digested (Roche; Indianapolis, IN) and then resolved on 10% SDS-PAGE as described in our published protocols [16]. For assessment of the total PrP, glial fibrillary acidic protein (GFAP) and various MCs, non-PK treated samples of brain homogenates containing 20μg of total protein were resolved on 10% SDS-PAGE and electroblotted into nitrocellulose membranes. The membranes were blocked with 5% nonfat milk in TBS-T for 1 h at room temperature and then incubated with commercially available, previously characterized primary monoclonal antibodies (mAbs) at the indicated dilutions: anti-PrP (clone 6D11 1:3,000, [19]), anti-GFAP (1:5,000), anti-Grp58 (1:1,000), anti-Grp78 (BiP; 1:1,000), anti-Grp94 (1:2,000), anti-HSP60 (1:4,000), anti-HSP70 (1:2,000), anti-HSP90 (1:1,000). All mAbs were obtained from Stressgen Bioreagents (Farmingdale, NY), except for 6D11 and anti-GFAP, which were provided by Dr. R.J. Kascsak (NYS Institute for Basic Research, Staten Island, NY) and purchased from Sigma (St. Lois, MO), respectively. The antigen-antibody complexes were detected using horseradish peroxidase-conjugated anti-mouse/rabbit/rat IgG (GE Healthcare Bio-Sciences Corp. Piscataway, NJ) and visualized using SuperSignal (Pierce Chemical; Rockford, IL). For each densitometrically analyzed protein all brain homogenate samples were electrophoresed and immunonoblotted at the same time, rigorously maintaining the same experimental conditions. Western immunoblots were digitized and subjected to densitometric analysis following our published protocols [16;19].

2.3. Histology

Paraffin embedded brain hemispheres were cut into coronal 12μm-thick sections, which were then carried on histological slides, deparaffinized, and stained with 1) hematoxylin-eosin for general neuropathological evaluation, which included assessment of spongiform pathology, 2) Thioflavin-S for amyloid plaques, or 3) immunostained with anti-GFAP mAbs (1:1,000) followed by Mouse on Mouse peroxidase kit (Vector Laboratories, Ltd. (Burlingame, CA) for assessment of astrogliosis [19].

2.5. Statistical Analysis

Mann-Whitney U test was used for pair-wise comparison of brain steady state levels of total PrP, PrP^{Sc}, GFAP, and various MCs among analyzed animal groups.

Results

All prion infected mice showed a significant elevation of the total PrP level comparing to the NBH-inoculated control mice. The PrP level ranged from 2.5±0.2 (mean±standard error of the mean) fold increase over the NBH-inoculated controls in 139A infected animals to 6.8±1.9 fold increase in 22L infected animals ($p<0.01$ vs. NBH; Fig 1A). There was also a modest but statistically significant 1.4 fold elevation of the total PrP level in both two and eight months old APPPS1-21 Tg mice over the NBH-inoculated mice ($p<0.01$). Following

the PK digestion PrP^{Sc} was detectable only in the brain homogenates of prion infected animals, with the lowest level observed in mice infected with 139A strain. Levels of PrP^{Sc} in brains of mice infected with ME7, 22L, and 87V strains were significantly higher than that in 139A infected mice by 1.7±0.2, 2.2±0.3 and 2.9±0.3 fold, respectively ($p<0.05$, Fig 1B).

As robust astrogliosis is a hallmark of neurodegeneration associated with prionoses, we quantified the steady-state level of GFAP in brains of mice infected with various prion strains and compared them to the NBH-inoculated controls. The increase in GFAP level ranged from 2.8±0.4 fold over the NBH-inoculated controls in 139A infected mice to 4.5±1.1 fold in ME7 infected mice ($p<0.05$; Fig 1C). Insignificant increase in GFAP level was seen in two months old APPPS1-21 Tg mice, while in eight months old APPPS1-21 mice the GFAP level was 3.1±0.6 higher than that in the NBH-inoculated animals ($p<0.05$).

The level of HSP60 was increased in the brains of ME7 and 87V infected mice by 1.3±0.02 fold and 1.4±0.01 fold comparing to the NBH-inoculated controls, respectively ($p<0.05$; Fig 1E). In contrast, in 22L and 139A infected mice the HSP60 level was reduced to 0.8±0.02 and 0.7±0.2 of the controls level, respectively ($p<0.05$). HSP60 was also significantly upregulated in two and eight months old APPPS1-21 mice by 1.3±0.1 and 1.5±0.1 fold, respectively ($p<0.05$). A robust HSP70 and HSP90 response was associated with all analyzed prion strains and it was also noticed in APPPS1-21 mice. The levels of both proteins were significantly higher in mice infected with ME7 and 87V strains and in two and eight months old APPPS1-21 mice, than in mice infected with 22L and 139A strains. In ME7 and 87V infected mice HSP70 showed 4.8±0.2 and 5.1±0.3 fold increase over the NBH-inoculated controls, respectively ($p<0.05;$ Fig 1F); while in two and eight months old APPPS1-21 mice the increase was 5.6±1.0 and 6.4±0.7 fold, respectively ($p<0.05$). In 22L and 139A infected mice HSP70 levels were 4.1±0.3 and 3.7±0.3 fold greater than that in the NBH-inoculated controls, respectively ($p<0.05$). The HSP90 level showed 3.3±0.7 and 6.0±1.4 fold increase in ME7 and 87V infected mice, respectively ($p<0.01$; Fig 1G); while in two and eight months old APPPS1-21 mice its level was 4.8±1.0 and 6.5±1.5 fold higher comparing to that in the NBH-inoculated controls, respectively ($p<0.01$). In 22L and 139A infected mice the HSP90 level was 2.8±0.6 and 2.0±0.2 fold greater than that in the NBH-inoculated controls, respectively ($p<0.01$).

Significant upregulation of Grp58 was associated only with 22L and 139A strains, where its steady-state level was 1.4±0.2 and 1.9±0.3 fold higher than that in the NBH-inoculated controls, respectively ($p<0.01$; Fig 1H). In mice infected with other prion strains and APPPS1-21 mice the level of Grp58 showed no statistically significant differences from the NBH-inoculated control animals. In contrast, Grp78 and Grp94 were upregulated in mice infected with ME7 and 87V strains and in APPPS1-21 AD Tg mice, whereas their levels showed no significant changes in mice infected with 22L and 139A strains. In mice infected with ME7 and 87V strains Grp78 level was 3.9±0.7 and 3.3±0.4 fold increased over the NBH-inoculated controls, respectively ($p<0.01$; Fig 1I); while in two and eight months old APPPS1-21 mice the increase was 2.7±0.1 and 3.6±0.8 fold, respectively ($p<0.01$). The Grp94 steady state level in ME7 and 87V infected mice was 4.4±0.3 and 8.3±0.2 fold higher than in the control, respectively ($p<0.05$; Fig 1J); and markedly contrasted with the steady state level of Grp94 in 22L and 139A infected mice, which was 1.1±0.3 and 1.0±0.3 of the mean control level, respectively ($p<0.05$; Fig 1J). In APPPS1-21 mice the Grp94 level was also markedly elevated akin to those observed in ME7 and 87V infected animals and it was 4.1±0.5 and 10.2±0.4 of the mean control level in two and eight months old animals, respectively ($p<0.05$ vs control, 22L and 139A). The difference between two and eight months old APPPS1-21 AD Tg mice was statistically significant ($p<0.05$).

Histopathological analysis revealed presence of Thioflavin-S positive amyloid plaques in the neocortex and the hippocampus of mice infected with ME7 and 87V strains but not in those infected with 22L and 139A strains or in control animals inoculated with NBH (Fig 1K). In mice infected with 87V strain the burden of amyloid plaques was somewhat greater and more consistent on serial rostro-caudal cortical sections than in mice infected with ME7 strain, where the burden was only occasionally matching that seen in 87V infected animals. Thioflavin-S positive Aβ plaques were also seen in the neocortex but not in the hippocampus of two months old APPPS1-21 Tg mice. The burden of amyloid plaques in the neocortex of two months old APPPS1-21 varied between animals but overall it was somewhat higher than the plaque burden in 87V infected mice. In eight months old APPPS1-21 Tg mice there was a substantial amyloid plaque burden both in the hippocampus and in the neocortex, which was incomparably higher to those, observed in younger Tg animals and in ME7 and 87V infected mice.

Various degree of spongiform changes was seen in the cortex of mice infected with all prion strains, but not those inoculated with NBH or in APPPS1-21 Tg mice (not shown). Robust astrogliosis, revealed by anti-GFAP immunohistochemistry was associated with all analyzed prion strains but it was not seen in the control NBH-inoculated mice. This observation was consistent with increase in the steady-state GFAP level demonstrated by Western-immunoblotting (Fig 1C). Reactive astrogliosis in prion infected mice showed mainly diffuse pattern while in mice infected with ME7 and 87V there were also visible clusters of astrocytes corresponding to the presence of amyloid deposits. Numerous reactive astrocytes, present mainly in the form of astrocytic clusters corresponding to amyloid Aβ plaques were also seen in eight month old APPPS1-21 AD Tg mice (not show).

Discussion

Although conformational transformation of PrP^{C} into β-sheet rich PrP^{Sc} is widely accepted as the underlying pathomechanism of prionoses, what governs phenotypical differences among prion strains remains an unsolved puzzle. The most prevailing hypothesis proposing how abnormal conformer of the same prion protein can give rise to a variety of phenotypically divergent strains, which can be faithfully reproduced after their passage, assumes existence of subtle conformational differences in PrP^{Sc} which are then adopted by the host PrP^{C} [26]. As MCs are intimately involved in preventing misfolding of client proteins and facilitate degradation of their misfolded conformers, we anticipated that their steady-state levels would be altered in infectious models of murine prionoses. Surprisingly, we found differences in how various mouse adapted scrapie strains engage MCs response. One common pattern was associated with ME7 and 87V strains and included upregulation of HSP60, HSP70, HSP90, Grp78, and Grp94 levels but not Grp58 level. Distinctly different pattern was associated with 22L and 139A strains where HSP60 level was down regulated, HSP70 and HSP90 levels showed increase, although significantly less pronounced than that associated with ME7 and 87V strains, Grp58 level was upregulated, while Grp78 and Grp94 levels showed no significant alterations. This different MCs response pattern was not directly associated with the brain concentration of PrP^{Sc} which was the lowest in 139A infected mice and the highest in mice infected with 87V and 22L strains. One common neuropathological feature distinguishing both ME7 and 87V strains from 22L and 139A strains is a propensity to form amyloid deposits composed of PrP protein. Beside selected mouse adapted scrapie strains, amyloidogenesis is present in some inherited forms of human prionoses (eg. Gerstmann-Sträussler-Scheinker syndrome associated with P102L or A117V PrP mutations), it can be encountered in 5–10% of patients with sporadic Creutzfeldt-Jakob disease (CJD), and is a hallmark of neuropathological picture of kuru and variant CJD, both of which are examples of transmissible prionoses in humans [9]. Why amyloidogenesis occurs only in a subset of prionoses still requires final explanation but it is well established

that the same amyloidogenic prion strain may produce variable plaque load, when transmitted to mice of different genetic backgrounds [4]. Infection of MB mice with 87V strain invariably produces robust amyloid deposition in all cases, while the number of amyloid bearing animals and the load of amyloid plaque resulting from the ME7 infection ranges between mouse strains. 22L and 139A strains are not associated with amyloid deposition regardless of mouse genetic background, but interestingly in mice expressing anchorless PrP protein 22L infection results in formation of numerous amyloid plaques, which suggests that disengagement of PrP from its cell membrane anchor is a prerequisite for amyloid formation [7]. Furthermore, APPPS1-21 AD Tg mice, which feature robust deposition of fibrillar Aβ, shared with ME7 and 22L infected mice similar MCs response pattern, which is another argument that variability in the pattern of MCs engagement is associated with amyloidogenic nature of some prion strains. Comparison between two and eight months old APPPS1-21 Tg mice, showed a trend for increased steady state expression level of all amyloid associated MCs in the older mice, which also had higher burden of amyloid deposits. The only statistically significant difference was observed for Grp94. Similarly comparison between mice infected with amyloidogenic prion strains ME7 and 87V showed higher steady state level of HSP90 (difference statistically insignificant) and Grp94 ($p<0.05$) in the later, in which presence of amyloid deposits was more consistent.

Several studies used cDNA microarrays to look into changes in gene expression profile during prion infection (reviewed in [3]). Although the primary focus of these studies was not profiling MCs as a gene class, similar to our findings up regulation of HSP70 gene was found both in mice infected with mouse adapted scrapie strains [23] and in rocky mountain elk infected with chronic wasting disease, which also showed up regulation of HSP110 [2]. Expression of HSP40 was found to be down regulated in the former study and up regulated in the latter.

Differential engagement of particular MCs in infectious models of prionoses and APPPS1-21 AD Tg mice can be also tied to their specific function and subcellular localization. HSP60 is a mitochondrial marker, which was modestly upregulated in mice infected with ME7 and 87V strains and in APPPS1-21 AD Tg mice but not in mice infected with 22L and 139A strains. Mitochondrial dysfunction was demonstrated to be associated with early stages of pathology caused by ME7 infection [20] and there is also evidence to indicate mitochondrial PrP^{Sc} accumulation [1]. Intramitochondrial accumulation of Aβ and functional impairment of mitochondria are well described phenomena in the course of AD pathophysiology [25]. Thus HSP60 upregulation reflects mitochondrial stress in disorders of misfolded proteins, more so in models of amylodoidogenic prionoses and AD Tg mice.

HSP70 and HSP90 comprise a major mechanism protecting cytosolic milieu against disturbed proteostasis. HSP70 binds abnormally folded proteins and directs them either for protesomal degradation or toward HSP90, which facilitates refolding. Consistent with these functions, there was a remarkable up regulation of both proteins in prion infected mice and in APPPS1-21 mice, with significantly higher response associated with amyloidogenic than non-amyloidogenic prion strains. HSP70 and HSP90 responses likely reflects previously described accumulation of PrP and Aβ aggregates in the cytosol of diseased neurons [5;11].

Grp family are ER resident proteins readily responding to stress induced by accumulation of misfolded proteins in the ER. The ER has been postulated to constitute one of cellular compartments contributing to PrP^{Sc} formation not only in hereditary prionoses but also in their transmissible forms (reviewed in [5]). We noticed selective upregulation of Grp58 associated with 22L and 139A strains while Grp78 and Grp94 were selectively upregulated in ME7 and 87V infected mice and in APPPS1-21 mice. Grp78 binds most of nascent proteins translated in the ER including PrP and aid their proper folding. In cellular models of

hereditary prionoses Grp78 was found to cause retention of misfolded PrP mutant in the ER and directed it for proteasomal degradation [14]. Irrespectively to chaperoning ER protein folding Grp78 together with Grp94 constitute high capacity/low affinity Ca^{2+} buffer critical for maintaining Ca^{2+} homeostasis in this compartment [24]. Recent evidence indicate that PrP misfolding in cellular models relevant to both infectious and hereditary prionoses affect ER Ca^{2+} homeostasis and sensitize cells to endoplasmic reticulum stress [27]. Impaired intraneuronal Ca^{2+} homeostasis, including increased ER Ca^{2+} store levels is also a hallmark of AD pathogenesis and akin to our findings in APPPS1-21 mice upregulation of Grp78 was also described in two months old 3×Tg-AD tg mice in association with intraneuronal presence of Aβ aggregates [22]. Grp58 is a disulfide isomerase, which was shown to bind PrP^{Sc} and prevent apoptosis through inhibiting caspase-12 activation [13]. Similar to our findings upregulation of Grp58 was reported in 139A infected mice in the past [13]. It is likely that mechanisms of ER stress in prionoses are complex and include accumulation of intracellular PrP^{Sc} aggregates, disturbance of Ca^{2+} homeostasis and induction of apoptosis. Differential upregulation of particular members of Grp family associated with different prion strains may indicate that one of these mechanisms could play more prominent role over others in a pathobiology of a given strain. Limited human data indicate upregulation of all three Grp58, Grp78, and Grp94 proteins in subjects who succumbed to sporadic and variant CJD [12].

5. Conclusions

MCs are invariably involved in pathobiology of prionoses but provided here evidence indicates that various mouse adapted scrapie strains engage MCs response differently, which may contribute importantly to phenotypical differences among prion strains. Amyloidogenic vs. non-amyloidogenic nature of prion strains appears to be an important factor driving response of particular MCs. Modulation of MCs expression is being explored as a therapeutic approach for various neurodegenerative disorders associated with accumulation of misfolded proteins [10;15]. Knowledge about involvement of particular MCs in pathogenesis of prionoses may provide important information in designing therapeutic strategies to improve their outcomes.

Acknowledgments

Grant support: NIRG-10-173233 (A.A.A.), NIRG-09-132224 (J.P.), IIRG-08-90630, R01AG029635, and K02AG034176 (M.J.S). The authors would like to acknowledge Dr. Mathias Jucker from Hertie-Institute for Clinical Brain Research, University of Tübingen (Tübingen, Germany) for providing APPPS1-21 mice and Dr. Richard R. Kascsak from the NYS Institute for Basic Research in Developmental Disabilities (Staten Island, NY) for providing 6D11 mAb.

References

1. Aiken JM, Williamson JL, Marsh RF. Evidence of mitochondrial involvement in scrapie infection. J Virol. 1989; 63:1686–1694. [PubMed: 2564438]
2. Basu U, Almeida LM, Dudas S, Graham CE, Czub S, Moore SS, Guan lL. Gene expression alterations in Rocky Mountain elk infected with chronic wasting disease. Prion. 2012; 6:282–301. [PubMed: 22561165]
3. Benetti F, Gasperini L, Zampieri M, Legname G. Gene expression profiling to identify druggable targets in prion diseases. Expert. Opin. Drug Discov. 2010; 5:177–202. [PubMed: 22822917]
4. Bruce ME, Dickinson AG, Fraser H. Cerebral amyloidosis in scrapie in the mouse: effect of agent strain and mouse genotype. J. Neuropathol. Exp. Neurol. 1976:471–478.
5. Campana V, Sarnataro D, Zurzolo C. The highways and byways of prion protein trafficking. Trends Cell Biol. 2005; 15:102–111. [PubMed: 15695097]

6. Carp RI, Moretz RC, Natelli M, Dickinson AG. Genetic control of scrapie: incubation period and plaque formation in I mice. J. Gen. Virol. 1987; 68:401–407. [PubMed: 3102684]
7. Chesebro B, Trifilo M, Race R, Meade-White K, Teng C, LaCasse R, Raymond L, Favara C, Baron G, Priola S, Caughey B, Masliah E, Oldstone M. Anchorless prion protein results in infectious amyloid disease without clinical scrapie. Science. 2005; 308:1435–1439. [PubMed: 15933194]
8. Cunningham C, Deacon RM, Chan K, Boche D, Rawlins JN, Perry VH. Neuropathologically distinct prion strains give rise to similar temporal profiles of behavioral deficits. Neurobiol. Dis. 2005; 18:258–269. [PubMed: 15686954]
9. DeArmond, SJ.; Kretzschmar, H.; Prusiner, SB. Prion diseases. In: Graham, DI.; Lantos, P., editors. Greenfield's Neuropathology. London: Arnold; 2002. p. 273-324.
10. Gestwicki JE, Garza D. Protein quality control in neurodegenerative disease. Prog. Mol. Biol. Transl. Sci. 2012; 107:327–353. [PubMed: 22482455]
11. Gouras GK, Tampellini D, Takahashi RH, Capetillo-Zarate E. Intraneuronal beta-amyloid accumulation and synapse pathology in Alzheimer's disease. Acta Neuropathol. 2010; 119:523–541. [PubMed: 20354705]
12. Hetz C, Russelakis-Carneiro M, Maundrell K, Castilla J, Soto C. Caspase-12 and endoplasmic reticulum stress mediate neurotoxicity of pathological prion protein. EMBO J. 2003; 22:5435–5445. [PubMed: 14532116]
13. Hetz C, Russelakis-Carneiro M, Walchli S, Carboni S, Vial-Knecht E, Maundrell K, Castilla J, Soto C. The disulfide isomerase Grp58 is a protective factor against prion neurotoxicity. J Neurosci. 2005; 25:2793–2802. [PubMed: 15772339]
14. Jin T, Gu Y, Zanusso G, Sy M, Kumar A, Cohen M, Gambetti P, Singh N. The chaperone protein BiP binds to a mutant prion protein and mediates its degradation by the proteasome. J Biol. Chem. 2000; 275:38699–38704. [PubMed: 10970892]
15. Kastle M, Grune T. Interactions of the proteasomal system with chaperones: protein triage and protein quality control. Prog. Mol. Biol. Transl. Sci. 2012; 109:113–160. [PubMed: 22727421]
16. Pankiewicz J, Prelli F, Sy MS, Kascsak RJ, Kascsak RB, Spinner DS, Carp RI, Meeker HC, Sadowski M, Wisniewski T. Clearance and prevention of prion infection in cell culture by anti-PrP antibodies. Eur. J. Neurosci. 2006; 23:2635–2647. [PubMed: 16817866]
17. Radde R, Bolmont T, Kaeser SA, Coomaraswamy J, Lindau D, Stoltze L, Calhoun ME, Jaggi F, Wolburg H, Gengler S, Haass C, Ghetti B, Czech C, Holscher C, Mathews PM, Jucker M. Aβ42-driven cerebral amyloidosis in transgenic mice reveals early and robust pathology. Embo Reports. 2006; 7:940–946. [PubMed: 16906128]
18. Sadowski M, Pankiewicz J, Scholtzova H, Tsai J, Li YS, Carp RI, Meeker HC, Gambetti P, Debnath M, Mathis CA, Shao L, Gan WB, Klunk WE, Wisniewski T. Targeting prion amyloid deposits in vivo. J. Neuropath. Exp. Neurol. 2004; 63:775–784. [PubMed: 15290902]
19. Sadowski MJ, Pankiewicz J, Prelli F, Scholtzova H, Spinner DS, Kascsak RB, Kascsak RJ, Wisniewski T. Anti-PrP Mab 6D11 Suppresses PrP^{Sc} Replication in Prion Infected Myeloid Precursor Line FDC-P1/22L and in the Lymphoreticular System In Vivo. Neurobiol Dis. 2009; 34:267–278. [PubMed: 19385058]
20. Siskova Z, Mahad DJ, Pudney C, Campbell G, Cadogan M, Asuni A, O'Connor V, Perry VH. Morphological and functional abnormalities in mitochondria associated with synaptic degeneration in prion disease. Am. J Pathol. 2010; 177:1411–1421. [PubMed: 20651247]
21. Sitia R, Braakman I. Quality control in the endoplasmic reticulum protein factory. Nature. 2003; 426:891–894. [PubMed: 14685249]
22. Soejima, N.; Ohyagi, Y.; Nakamura, N.; Himeno, E.; Iinuma, KM.; Sakae, N.; Yamasaki, R.; Tabira, T.; Murakami, K.; Irie, K.; Kinoshita, N.; LaFerla, FM.; Kiyohara, Y.; Toru, I.; Kira, JI. Intracellular Accumulation of Toxic Turn Amyloid-beta is Associated with Endoplasmic Reticulum Stress in Alzheimer's disease. Curr. Alzheimer Res. Epub ahead of print (http://www.ncbi.nlm.nih.gov/pubmed/22950910).
23. Sorensen G, Medina S, Parchaliuk D, Phillipson C, Robertson C, Booth SA. Comprehensive transcriptional profiling of prion infection in mouse models reveals networks of responsive genes. BMC. Genomics. 2008; 9:114. [PubMed: 18315872]

24. Stutzmann GE, Mattson MP. Endoplasmic reticulum Ca(2+) handling in excitable cells in health and disease. Pharmacol. Rev. 2011; 63:700–727. [PubMed: 21737534]

25. Takuma K, Fang F, Zhang W, Yan S, Fukuzaki E, Du H, Sosunov A, McKhann G, Funatsu Y, Nakamichi N, Nagai T, Mizoguchi H, Ibi D, Hori O, Ogawa S, Stern DM, Yamada K, Yan SS. RAGE-mediated signaling contributes to intraneuronal transport of amyloid-beta and neuronal dysfunction. Proc. Natl. Acad. Sci. U. S. A. 2009; 106:20021–20026. [PubMed: 19901339]

26. Thackray AM, Hopkins L, Klein MA, Bujdoso R. Mouse-adapted ovine scrapie prion strains are characterized by different conformers of PrP^{Sc}. J. Virol. 2007; 81:12119–12127. [PubMed: 17728226]

27. Torres M, Castillo K, Armisen R, Stutzin A, Soto C, Hetz C. Prion protein misfolding affects calcium homeostasis and sensitizes cells to endoplasmic reticulum stress. PLoS. One. 2010; 5:e15658. [PubMed: 21209925]

Research highlights

- ✓ Molecular chaperones (MCs) such as HSPs and Grps are involved in prion diseases.
- ✓ Various mouse adapted scrapie strains produce differential MCs response.
- ✓ Amyloidogenic and non-amyloidogenic prion strains engage MCs differently.
- ✓ MCs response in amyloidogenic prion strains and APPPS1-21 AD Tg mice is similar.

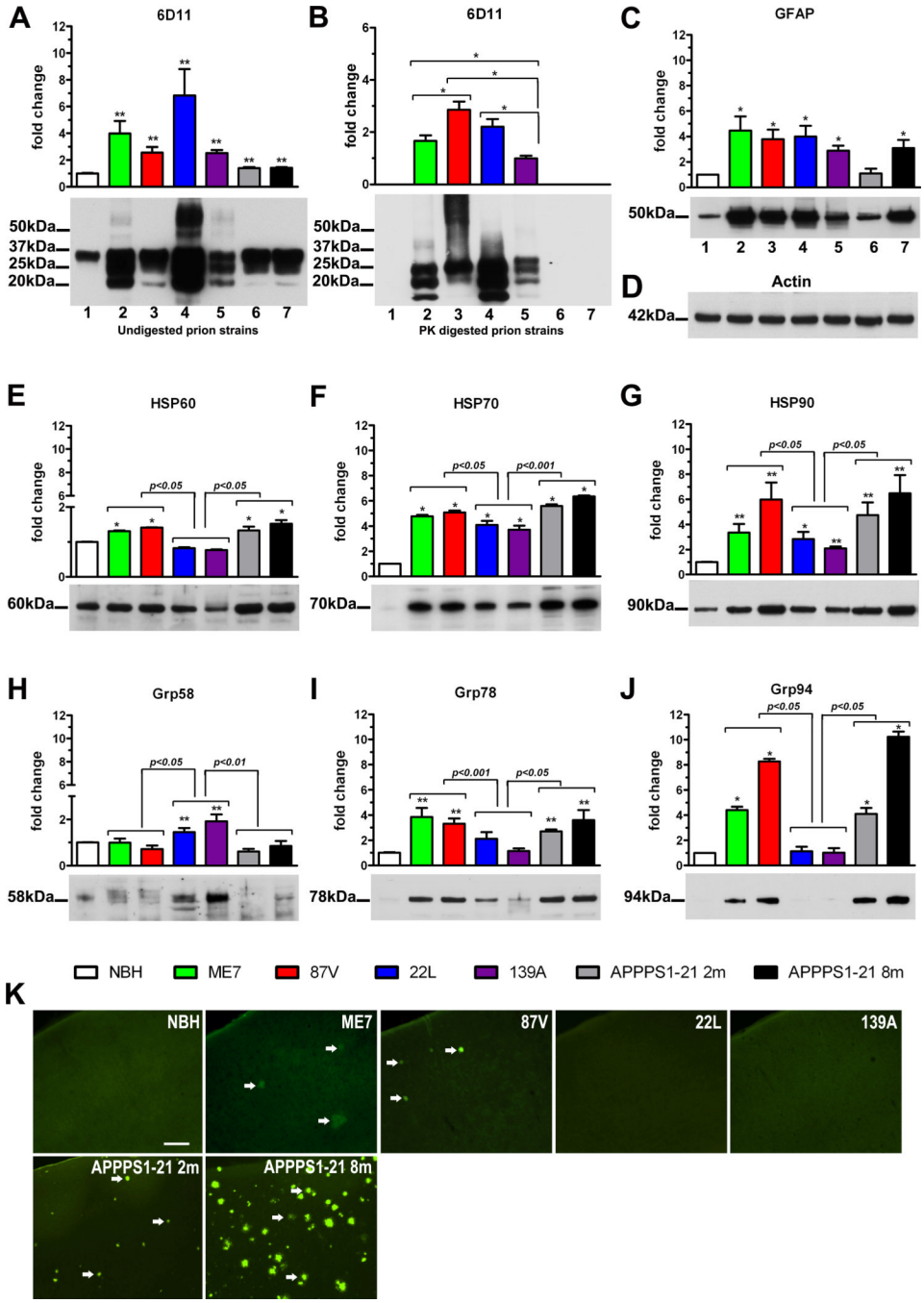

Figure 1.

Biochemical and histological analysis of brains from NBH-inoculated control mice; mice inoculated with ME7, 87V, 139A, and 22L prion strains; and two (2m) and eight (8m) months old APPPS1-21 AD Tg mice. Biochemistry: densitometric analysis (n=6 per group) and representative Western immunoblots profiling the steady-state levels of total PrP **(A)**, PrP^{Sc} **(B)**; GFAP **(C)**, actin (**D**, used as the loading control), HSP60 **(E)**; HSP70 **(F)**; HSP90 **(G)**; Grp58 **(H)**; Grp78 **(I)**, and Grp94 **(J)**. Values in the graphs show the mean fold change of band intensities (±SEM) analyzed by densitometry relative to those in the control NBH-inoculated animals, except for (C) which shows the mean fold change of band intensities

relative to those in 139A infected animals. The average band density in the control NBH-inoculated animals used as a reference value was calculated for each protein separately. Asterisks above the bars denote results of pair-wise comparison against the control NBH-inoculated mice: * $p<0.05$, ** $p<0.01$. Results of comparison between pairs of amyloidogenic ME7 and 87V prion strains, APPPS1-21 mice and non-amyloidogenic 139A and 22L prion strains are shown directly above the brackets spanning the groups. The position of protein size markers next to Western immunoblots are indicated in thousand of Daltons (kDa). Histology: **(K)** representative images of coronal sections through S1 cortical area stained with Thioflavin-S. Arrows indentify Thioflavin-S binding amyloid plaques. Scale bar =100μm.